Adaptive Model Predictive Control for a Magnetic Suspension System under Initial Position Dispersions and Voltage Disturbances

Fawaz F. Al-Bakri
University of Babylon
College of Engineering, Biomedical Engineering Department
Iraq

Salwan Obaid Waheed Kafaji
University of Babylon
College of Engineering, Mechanical Engineering Department
Iraq

Hasan H. Ali
Directorate of Reconstruction and Projects
Ministry of Higher Education and Scientific Research
Iraq

A nonlinear magnetic suspension system consisting of a mechanical motion and electromagnetic circuit is considered in this paper. An online algorithm that is used to stabilize the suspended mass targeting the desired ball position, ball velocity and coil current is presented. A steady-state condition, in which the ball position, the ball velocity, and the coil current were assumed constant, was used as a reference trajectory for the closed-loop simulations. An adaptive model predictive control method was employed to control the coil voltage while the discrete plant model and operating conditions were changed at each time step. The effectiveness of the proposed control law was validated in the presence of disturbances in initial ball position, steady-state ball position, suspended mass, and voltage using the Monte-Carlo simulation method. The sinusoidal, step, and impulse voltage disturbances were applied consequently to the system while imposing random dispersions of the initial ball position. Numerical results with five hundred trials illustrated that the designed algorithm can stabilize the system and track the desired reference without exceeding the state and input constraints despite the wide range of dispersions in initial ball position, steady-state ball position, suspended mass, and input voltage disturbances.

Keywords: *Predictive control, magnetic, suspension system, voltage disturbance, Monte-Carlo simulation.*

1. INTRODUCTION

The magnetic levitation and suspension systems can be used to reduce the friction between moving surfaces. These systems attracted researchers' attention due to their wide range of applications. A lot of applications have been presented in the literature showing that magnetic levitation is used to improve efficiency. For example, it is used for trains of high speed [1], magnetic bearing [2], a gyroscopic suspension system [3], wind turbine [4, 5], vibration isolation, quick response tool applications [6-8], and space mission for launch assistance system [9].

The magnetic levitation system presents a non-mechanical contact force as a magnetic force developed in the air gap and that motivated the researchers to pay more attention regarding using it in numeral applications. However, the problem of controlling the position throughout these systems has been representing the main challenge. The theories of classical control have presented several designs for this purpose. However, ensuring steady and smooth performance was not quarantined because of using the classical strategies of constant linear control which failed rapidly because of deviation from the normal response. Furthermore, because of the inherent nonlinearities and the open-loop insatiability feature of the magnetic suspension system, the development of a high-performance design for controlling the position became critical. In addition, the controller, usually, for these systems is designed to ensure the levitated part to be closer to the nominal and desired value, otherwise, the controller performance will be hindered by either system nonlinearities or distur–bance in the system input (voltage, as an example). The first attempts of the design methods for the linear and nonlinear feedback controllers were noticed in 1996 and 2001 by Baire and Chiasson [10] and El Haj-jaji and Ouladsine [11], respectively. These methods were built based on feedback linearization [12].

Other techniques of the feedback linearization cont–rol were reported by many researchers [13-16]. How–ever, in [13] and [14], those techniques were imple–mented for transforming the model of the magnetic systems into a comparable and equivalent model with a simpler model. Within the simplified models of the magnetic suspension systems, only the nominal para–meters of the systems were taken into account in the design of the feedback linearization. This usually re–sulted in the presence of instability and performance depreciated because of the variations of the system parameters due to the thermal losses. In [17], the system nonlinearity was approximated by using Taylor's series expansion with reduced orders only, where the higher-order terms were neglected and that affected the

Received: May 2021, Accepted: December 2021
Correspondence to: Dr. Salwan Obaid Waheed Khafaji
College of Mechanical Engineering,
University of Babylon-Mechanical Eng. Dep. Iraq
E-mail: eng.salwon.obaid@uobabylon.edu.iq
doi: 10.5937/fme2201211A

modeling performance. The control system was guaranteed the systems theoretically, and relatively large oscillations and overshoots were noted in the transient analysis in the experimental test, especially with introducing uncertainties. Adaptive and robust controllers have been introduced in [18].

Nonlinear controller and quantitative feedback technique have been reported to design a 2-DOF controller to reduce the effect of the uncertainties in the system parameters [19, 20]. Therefore, developing a simple and efficient method for controlling the magnetic suspension system even in the presence of system uncertainty became necessary.

In recent years, sliding mode control has been presented, where the magnetic levitation system has been modeled as a second-order differential equation [21]. However, the experimental setup does not match the theoretical modeling because of the assumption of frictionless motion of the levitation object. That exhi–bited an oscillatory response toward the desired posi–tion. In addition, the response of the open-loop system showed an underdamped response which resulted in logarithmic decrement before getting the steady-state response (desired position). Therefore, it is important to design a controller that responds with no overshoots. In [22], the H-infinity controller was designed for a ball-plate system to stabilize the ball with specific per–formance characteristics. A robust controller was designed in [23] for magnetic suspension systems using the discontinuous integral method. Theoretical and experimental results showed that the designed controller was able to achieve good tracking characteristics for the magnetic suspension system. A homogenous discon–tinuous integral method was used in [24] to design a sliding mode robust controller that provides smooth and accurate tracking. The performance of the designed controller was assessed experimentally by applying it to a magnetic suspension system which confirmed its effectiveness of it. In [25], a flux path control was used to design a magnetic suspension system. A model was constructed and a proportional-derivative (PD) control–ler was designed. The results showed that when a small step or force disturbance is applied to the system, a new equilibrium position for the suspended ball will be reached under the real-time control system effect.

Several researchers have considered some algo–rithms to improve wind turbines performance [26] and [27]. In [26], a new algorithm to optimize a wind tur–bine position relying on a genetic optimization metho–dology was proposed. Using the presented technique, the aerodynamic wind model has been improved despite the effects of viscous fluid flow. While in [27], a fabrication of wind turbine rotor blades has been developed experimentally based on composite materials.

The proposed model was verified using CATIA and Gerber Garment systems.

The magnetic levitation has been utilized to compute well-suited aerodynamics coefficients for both transonic and subsonic aircraft. In [28], Subsonic wind tunnels supported by bent sting and external model were considered. The presented model has been tested under conditions that are significantly similar to aircraft real conditions. The simulated results have validated the experimental results to compute well-suited aircraft aerodynamic coefficients. In [29] and [30], T-35 4.4 m × 3.2 m and VTI's subsonic wind tunnels, respectively, were considered. The system performance was tested in the presence of wind tunnel and instruments calibrations. The results insured an effective performance compared to prior subsonic wind tunnel models. In [31], six wind tunnels with three transonic Mach numbers were considered. The simulated results illustrated reasonable drag polar coefficients at sonic Mach number compared with other transonic Mach numbers.

Other novel algorithms to stabilize magnetic sus–pension systems were considered. In [32], and analytical strategy to shape system references was proposed. The linear control method "Gain Shechting "was utilized to steer the suspended mass tracking the generated reference profiles in the presence of ball position disturbances.

Despite many prior works that have stabilized the magnetic levitation system numerically or optimally, several of these methods are not applicable or feasible to be solved in real-time as well as they cannot app–ropriately cope with wide disturbances of states and inputs.

This paper presents an online algorithm that utilizes steady-state conditions to generate the desired refe–rences. An adaptive model predictive control, which updates the system plant model at each time step, was used to create the coil voltage profile that tracks the reference profiles. The magnetic suspension system ro–bustness was considered when the system's initial ball position, steady-state ball position, suspended mass, and coil voltage experience uncertainty under the proposed control law. In this work, random initial ball position, steady-state ball position, suspended mass, and voltage signal disturbances were considered by using three types of input disturbances, sinusoidal, step, and im–pulse which fed consequently to the system. Monte-Carlo simulation method was used to demonstrate the effectiveness of the proposed algorithm

2. SYSTEM MODEL

The main goal of the magnetic suspension system is to stabilize and balance the suspended mass at a certain position while satisfying all the system constraints. In this work, the voltage was considered as a command (the control factor) to control the rigid body ball position. The schematic diagram of the magnetic suspension system, consisting of a mechanical motion and electric circuit, is shown in Fig. 1 [33]. Where m is the mass of the suspended ball, y is the position of the ball measured from a reference position ($y = 0$) and directed downward, i is the current in the coil, $f(y,i)$ is the magnetic force between the electromagnetic system and iron ball generated by the electric current (i), u is the control voltage, and g is the gravitational acce–leration.

The inductance (L) of the electromagnetic system can be described as a function of the ball position as follows [26],

$$L(y) = L_1 + \frac{aL_0}{(a+y)} \tag{1}$$

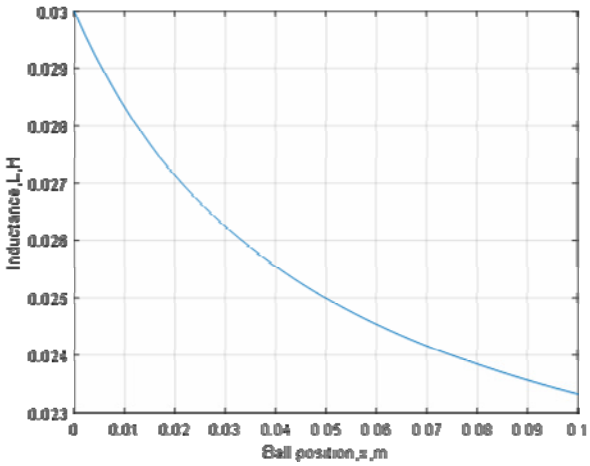

Figure 1: Magnetic Suspension System Model

Where L_0, L_1, and a should be positive constants to provide positive coil inductance. Clearly, Eq. (1) shows that the inductance increases to reach it maximum value ($L = L_1 + L_0$) when the ball is moved to (y =0) while it takes a minimum value ($L=L_1$) when the ball is located at the reference point ($y = \infty$). A profile of the proposed inductance is illustrated in Fig. 2.

The equation of the motion of the ball can be modeled using Newton's second law, so that:

$$m\ddot{y} = -k\dot{y} + mg - f(y,i) \tag{1}$$

where k is a viscous friction coefficient (not shown in Fig. 1 for simplicity).

The energy stored in the electromagnetic circuit can be easily computed by,

$$E(y,i) = \frac{1}{2}L(y)i^2 \tag{2}$$

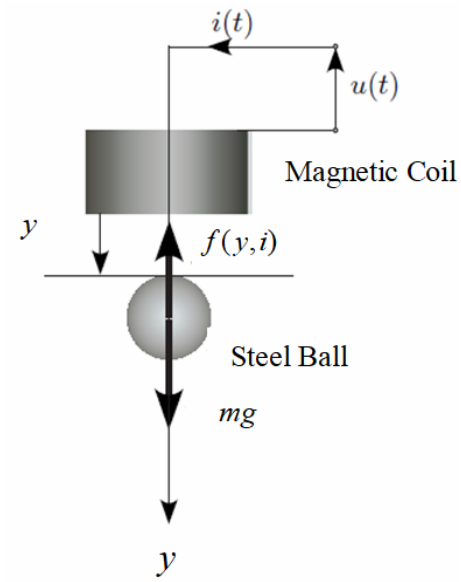

Figure 2: Inductance Profile

A simple way to find the generated magnetic force $f(y,i)$ can be accomplished by differentiating Eq. (3) concerning the ball position, so that:

$$f(y,i) == \frac{L_0 i^2}{2a(1+y/a)^2} \tag{3}$$

By applying Kirchhoff's voltage law, it is obtained,

$$V = \dot{\phi} + Ri \tag{2}$$

where ϕ is the magnetic flux linkage, which can be defined as,

$$\phi = L(y)i \tag{6}$$

The set of nonlinear models can be described as a state-space representation (SSR) formed by supposing $x = [x_1\ x_2\ x_3] = [y\ \dot{y}\ i]$ are the system states and $u = V$ is the system input as follows,

$$\dot{x}_1 = x_2$$

$$\dot{x}_2 = g - \frac{k}{m}x_2 - \frac{aL_0}{2m(a+x_1)^2}x_3^2 \tag{7}$$

$$\dot{x}_3 = \frac{1}{L(x_1)}\left(-Rx_3 + \frac{L_0}{(a+x_1)^2}x_2x_3 + v\right)$$

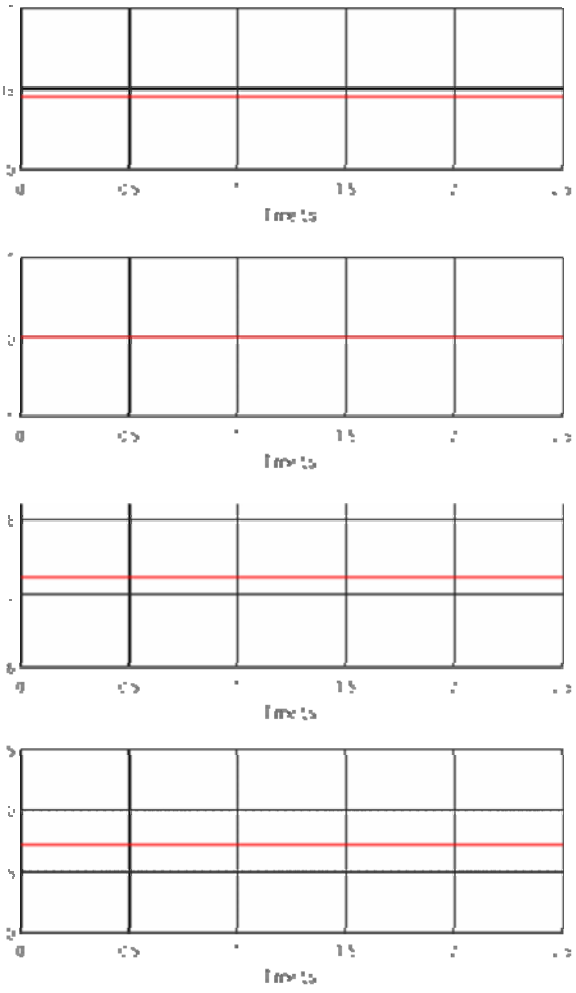

Figure 2. Reference magnetic profiles for m=0.15 kg and y0=0.04 m; (a) ball position vs. time; (b) ball velocity vs. time; (c) coil current vs. time; (d) coil voltage vs. time

Hence, the state space representation (SSR) can be expressed in a linear standard form as,

$$\begin{aligned} \dot{x} &= A_c(x)x + B_c(x)u \\ Y &= C_c x + D_c u \end{aligned} \tag{8}$$

$$A_c(x) = \sum_i^n \sum_j^n \frac{\partial f_i}{\partial x_j} = \begin{bmatrix} \frac{\partial f_1}{\partial x_1} & \cdots & \frac{\partial f_1}{\partial x_n} \\ \vdots & & \vdots \\ \frac{\partial f_n}{\partial x_1} & \cdots & \frac{\partial f_n}{\partial x_n} \end{bmatrix} \quad (9)$$

where $A_c \in \mathbb{R}^{n \times n}$, and

$$B_c(x) = \sum_i^n \sum_j^m \frac{\partial f_i}{\partial u_j} = \begin{bmatrix} \frac{\partial f_1}{\partial u_1} & \cdots & \frac{\partial f_1}{\partial u_m} \\ \vdots & & \vdots \\ \frac{\partial f_n}{\partial u_1} & \cdots & \frac{\partial f_n}{\partial u_m} \end{bmatrix} \quad (10)$$

where $B_c \in \mathbb{R}^{n \times m}$

The state-space representation model of the pro–posed system for three states (n =3) and one input (m =1) can be written as,

$$A = A_{11} = A_{13} = 0,\ A_{12} = 1$$

$$A_{21} = \frac{aL_0 x_3^2}{m(a+x_1)^3},$$

$$A_{22} = -\frac{k}{m},$$

$$A_{23} = -\frac{aL_0 x_3}{m(a+x_1)^2}$$

$$A_{31} = \left(\frac{\left\{ aL_0 \left(\begin{array}{l} Rx_1^2 x_3 - vx_1^2 - va^2 \\ -2avx_1 + Ra^2 x_3 + 2Rax_1 x_3 + \\ 2L_1 x_1 x_2 x_3 + aL_0 x_2 x_3 + 2aL_1 x_2 x_3 \end{array} \right) \right\}}{(a+x_1)^2 (aL_0 + aL_1 + L_1 x_1)^2} \right) \quad (11)$$

$$A_{32} = \left(\frac{aL_0 x_3}{(a+x_1)(aL_0 + aL_1 + L_1 x_1)} \right),$$

$$A_{33} = -\left(\frac{(Ra^2 + 2aRx_1 - aL_0 x_2 + Rx_1^2)}{(a+x_1)(aL_0 + aL_1 + L_1 x_1)} \right)$$

$$B_c(x) = \begin{bmatrix} 0 \\ 0 \\ \frac{(a+x_1)}{(aL_0 + aL_1 + L_1 x_1)} \end{bmatrix} \quad (12)$$

$$C_c = [0 \quad 0 \quad 1], \quad D_c = [0] \quad (13)$$

It is noted that the matrices are highly nonlinear in terms of the ball position, ball velocity, coil current, and coil voltage, while other system parameters are constant as shown in Table 1. The model is obtained as a continuous state-space model as described by Eqs. (10, 11, 12, and 13). However, in our work, a discrete-time state-space model is needed to model the controller. Thus, the discrete-time state space can be described as follows,

$$\left\{ \begin{array}{l} x(k+1) = A(x)x(k) + B(x)u(k) \\ Y(k) \quad\ = C\,x(k) + D\,u(k) \end{array} \right\} \quad (14)$$

where *A(x)* and *B(x)* are obtained by sampling the conti–nuous state-space system.

3. MAGNETIC SUSPENSION REFERENCE

The nonlinear system can be stabilized around either an equilibrium operating point or a specific trajectory. A steady-state condition, which assumes that the ball position, the ball velocity, and the coil current, are cons–tants, was used to generate a reference trajectory. The steady-state position was assumed to be known (y_{ss} = 0.045m). Hence, the steady-state conditions can easily be achieved by substituting $x_1 = y_{ss}$ and setting Eq. 7 to zero; therefore, the reference position, velocity, current, and voltage can be obtained respectively, as follows,

$$\left\{ \begin{array}{l} y_{ss} = 0.045m \\ v_{ss} = 0 \\ i_{ss} = \sqrt{\frac{2mg(a+y_{ss})^2}{aL_0}} \\ V_{ss} = Ri_{ss} \end{array} \right\} \quad (15)$$

Figures 3(a)-3(d), present the reference ball position, ball velocity, coil current, and coil voltage profiles, respectively. It is noticed from Fig.3 that all the reference states and input have constant values during the simulations and their values are: y_{ss}=0.045m, v_{ss}=0 m/s, i_{ss}=7.288 Amp, and V_{ss}=7.288 Volt.

4. ADAPTIVE MODEL PREDICTIVE CONTROL

The main purpose of this work is to stabilize the proposed magnetic suspension system around the steady-state profiles within 0.5 sec. We have presented an adaptive model predictive control (AMPC) to com–pute gains at each time step, while the discrete plant model and operating conditions are changing.

The AMPC is a powerful optimization strategy for feedback control based on a model of a system. This model runs forecast forward in time for different actuation strategies input to optimize the control over a short period. Essentially, this method determines the immediate next control action based on the opti–mization. Once the next control optimization has been applied, the optimization is reinitialized by moving the time window over to find the next control. These processes, essentially, keep matching that window forward and forward in time. The adaptive model predictive control is designed based on a model

predictive control; however, the proposed control method updates the discrete plant model and operating conditions at each time step. The model predictive control objective function can be formulated as [34]:

$$J(k)=\sum_{j=0}^{N-1}\begin{Bmatrix} x^T(k+j/k)Qx(k+j/k)+u^T(k+j/k) \\ \Re u(k+j/k)+x^T(k+N/k)Q_N\,x(k+N/k) \end{Bmatrix} \quad (16)$$

where the weight matrix for the state $Q\in\mathbb{R}^{n\times n}$ and the weight matrix for the input effort $\Re\in\mathbb{R}^{m\times m}$ is positive-semi definite and positive definite, respectively. The terminal weight matrix $Q_N\in\mathbb{R}^{n\times n}$ can be computed by solving the discrete-time Lyapunov equation [35],

$$\left[A(x)\text{-}B(x)k_{LQR}\right]X\left[A(x)\text{-}B(x)k_{LQR}\right]^T\text{-}X+Q_N(x)=0 \quad (17)$$

where k_{LQR} is the optimal gain vector obtained by using the Linear Quadratic Regulator (LQR) method [36] and [37].

The predicted states and input within using five prediction steps (N=5) can be expressed as shown in Eqs. (18) and (19), respectively.

$$X(k)=\begin{bmatrix} x^T(k+1|k),x^T(k+2|k), \\ x^T(k+3|k),x^T(k+4|k), \\ x^T(k+5|k) \end{bmatrix}^T \quad (18)$$

$$U(k)=\begin{bmatrix} u^T(k|k),u^T(k+1|k), \\ u^T(k+2|k),u^T(k+3|k), \\ u^T(k+4|k) \end{bmatrix}^T \quad (19)$$

where $X\in\mathbb{R}^{n\times N}$ and $U\in\mathbb{R}^{m\times N}$

Hence, the predicted state sequence is:

$$X(k)\ =\ M(k)x(k|k)+S(k)U(k) \quad (20)$$

$M(k)\in\mathbb{R}^{n\times N}\times\mathbb{R}^{n\times N}$ and $S(k)\in\mathbb{R}^{n\times N}\times\mathbb{R}^{m\times N}$ can be defined as,

$$M(k)=\left[A(x),A^2(x),A^3(x),A^4(x),A^5(x)\right]^T$$

$$S(k)=\begin{bmatrix} B(x) & 0 & 0 & 0 & 0 \\ A(x)B(x) & B(x) & 0 & 0 & 0 \\ A^2(x)B(x) & A(x)B(x) & B(x) & 0 & 0 \\ A^3(x)B(x) & A^2(x)B(x) & A(x)B(x) & B(x) & 0 \\ A^4(x)B(x) & A^3(x)B(x) & A^2(x)B(x) & A(x)B(x) & B(x) \end{bmatrix} \quad (21)$$

The block diagonal matrix ($\bar{Q}$) can be written based on the weighting matrix (Q) and the terminal weight matrix Q_N as follows,

$$\bar{Q}(x)=\begin{bmatrix} Q & 0 & 0 & 0 & 0 \\ 0 & Q & 0 & 0 & 0 \\ 0 & 0 & Q & 0 & 0 \\ 0 & 0 & 0 & Q & 0 \\ 0 & 0 & 0 & 0 & Q_N(x) \end{bmatrix} \quad (22)$$

where $\bar{Q}(k)\in\mathbb{R}^{n\times N}\times\mathbb{R}^{n\times N}$. In addition, the block diago–nal matrix ($\bar{R}$) can be written based on the weighting matrix ($\Re$) as follows,

$$\bar{R}=\begin{bmatrix} \Re & 0 & 0 & 0 & 0 \\ 0 & \Re & 0 & 0 & 0 \\ 0 & 0 & \Re & 0 & 0 \\ 0 & 0 & 0 & \Re & 0 \\ 0 & 0 & 0 & 0 & \Re \end{bmatrix} \quad (23)$$

$$\bar{J}(k)=U^T(k)HU(k)+2x^T(k|k)F^TU(k) \quad (24)$$

$$U(k)=\begin{bmatrix} u^T(k|k),u^T(k+1|k), \\ u^T(k+2|k),u^T(k+3|k), \\ u^T(k+4|k) \end{bmatrix}^T$$

where $\bar{R}\in\mathbb{R}^{m\times N}\times\mathbb{R}^{m\times N}$

It is convenient to convert the model predictive con–trol scenario into a standard Quadratic Programming (QP) one, which objective function can be obtained as follows,

$$H=S^T\bar{Q}S+\bar{R} \quad (25)$$

where $H\in\mathbb{R}^{m\times N}\times\mathbb{R}^{m\times N}$, is a positive definite Hessian matrix which can be obtained as follows, $F\in\mathbb{R}^{m\times N}$, is the linear part of the QP objective function and can be obtained as follows,

$$F=S^T\bar{Q}M \quad (26)$$

Hence, the model predictive gain can be computed by:

$$k_{MPC}=H^{-1}F \quad (27)$$

Then, the coil voltage can be evaluated as follows,

$$V=V_{ss}-k_{MPC}\begin{bmatrix} (x_1-y_{ss}) \\ x_2 \\ (x_3-i_{ss}) \end{bmatrix} \quad (28)$$

The first term of the model predictive control is used to stabilize the magnetic suspension system for tracking the reference ball position and steady-state current. The adaptive model predictive control is designed based on a model predictive control; however, the proposed control method updates the discrete plant model and operating conditions at each time step. Hence, all the model predictive control processes are required to be repeated in a specific order to update the control over a short period.

5. NUMERICAL RESULTS

The objective of dispersion trails is to evaluate the performance of the online magnetic algorithm in the presence of large perturbations in the initial ball position. Nominal and off-nominal simulations were tested by integrating the set of nonlinear model Eq. (7)

numerically using a fixed-step, Runge-Kutta solver (MATLAB's ode4). The coil voltage was computed using the steady-state (V_{ss}) and closed-loop commands to track the desired trajectory. It is important to mention that ball position and input voltage were constrained with upper and lower values. The ball position profile should be within the interval [0- 0.1] m while the input voltage profile is limited to be between [0-15] volt [26].

In summary, the steady-state condition was used to generate the reference trajectory for a known steady-state ball position Eq. (15). Then the closed-loop command was designed instantaneously based on the current discrete system and the operating conditions using the adaptive model predictive control Eq. (27). Finally, open and closed-loop commands were obtained to stabilize the suspended mass targeting the steady-state ball position, ball velocity, and coil current under nominal and off-nominal conditions Eq. (28).

6. RESULTS AND DISCUSSION

6.1 Nominal Conditions

The nominal initial conditions for the magnetic suspension system were taken from [33]. During the nominal simulation, there was no disturbance in the coil voltage and the nominal conditions were m= 0.15 kg and y0=0.04 m. Figures 4(a)-4(d), show the reference and nominal ball position, ball velocity, coil current, and coil voltage profiles, respectively. The red lines show the reference trajectories while the blue lines demonstrate the closed-loop nominal profiles using the adaptive model predictive. As mentioned previously, during the nominal simulation, no disturbance was applied to the input voltage. It is noted that the responses of all states were quite smooth and stable without exceeding the state and input constraints. The peak of the ball position response (overshoot) was relatively small and the system needed only 0.65 sec to reach the desired profile for all system states. The final state errors were very small because of the mechanism of the adaptive model predictive control, which iterated the response at each step time until gathering the converged response to the reference ball position. These results show the ability of the proposed control to get a fast response with limited input energy. However, it is unlikely to assess the effectiveness of the proposed algorithm without taking the off-nominal conditions into account.

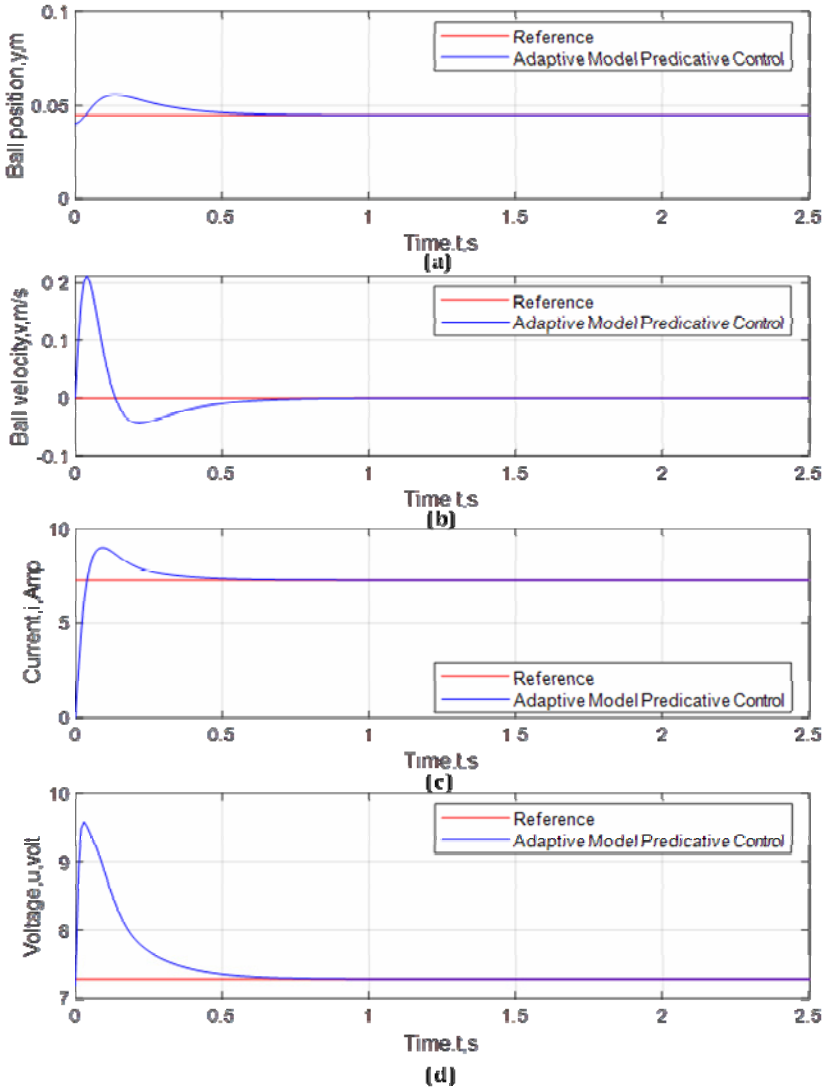

Figure 4. Nominal magnetic profiles for m=0.15 kg and y0=0.04 m without voltage disturbance; (a) ball position vs. time; (b) ball velocity vs. time; (c) coil current vs. time; (d) coil voltage vs. time

6.2 Off-Nominal Conditions

6.2.1 Initial Ball Position and Input Voltage disturbances

Many dispersed initial ball positions were tested to illustrate the robustness of the proposed magnetic suspension algorithm. In this work, we impose random initial ball position conditions and input voltage disturbances. Three disturbance functions, sinusoidal, step, and impulse were applied to the coil voltage after reaching the steady-state conditions. The off-nominal conditions of the initial position and voltage are shown in Tables 2 and 3, respectively.

Parametric uncertainty is not unusual in dynamic systems because these systems usually work under non-ideal conditions where the design parameters may change. Therefore, taking such changes into account, when designing a control system, is important [38]. Monte-Carlo simulation was utilized to perform the proposed online magnetic algorithm by considering 500 trials for each disturbance of the coil voltage as well as considering the random dispersions of initial ball positions as shown in Tables 2 and 3.

Table 2 Off-nominal initial position

Parameter	Max value (m)	Min value(m)
Initial Position	0	0.08

Table 3: Off-nominal voltage disturbances

Input voltage	Max freq. (H)	Min freq. (H)	Max ampl. (Volt)	Min ampl. (Volt)
Sinusoidal	20	5	0.25	0.05
Step	-	-	0.25	0.05
Impulse	-	-	0.25	0.05

The input disturbances were applied consequently to the system. The sinusoidal disturbance was added first to the coil voltage after reaching the steady-state conditions at t = 0.9 sec. Then the step disturbance was applied to the voltage between [1.1-1.15] sec, and eventually, the impulse disturbance was taken into account at t = 1.15 sec. This combination of the disturbance functions was employed to perform the ability of the proposed algorithm to stabilize the system quickly with a lower overshoot.

Figures 5(a)-5(c) present the 500 trials of ball position, ball velocity, coil current histories, respectively. These figures match the steady-state conditions well in the presence of large dispersions of initial ball position and voltage uncertainties. Figure 5(a) was obtained to be feasible because all of the ball position profiles track the references perfectly within the interval [0 - 0.1] m. Figure 5(d) shows 500 closed-loop voltage histories. As seen from Fig. 5(d), the steady-state time and overshoot vary due to the variation of system inputs. This figure shows that the actual trajectories track the steady-state references and satisfy the closed-loop voltage limitation [0-15v]. In addition, as the differences between the nominal and off-nominal values of the uncertain parameters become larger, the time required to reach the steady-state conditions increases.

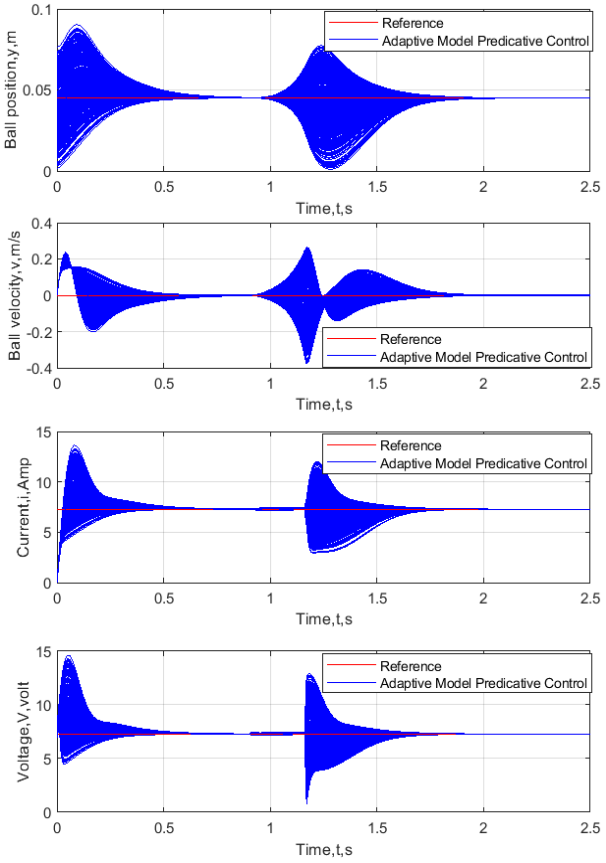

Figure (5) Off-nominal magnetic profiles with dispersions of initial ball position and voltage disturbance; (a) ball position vs. time; (b) ball velocity vs. time; (c) coil current vs. time; (d) coil voltage vs. time.

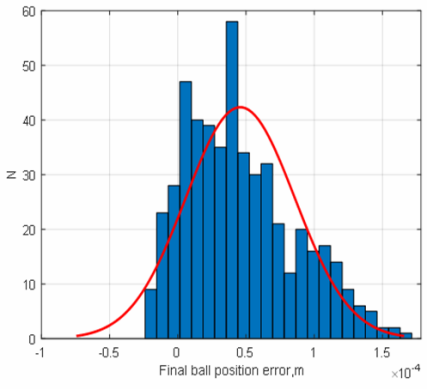

a)

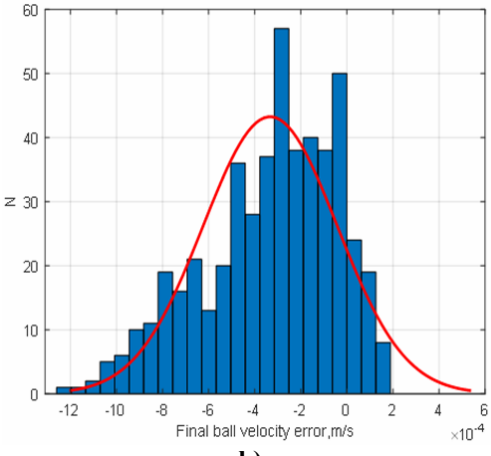

b)

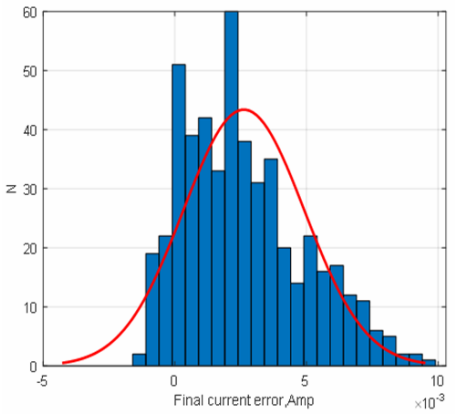

c)

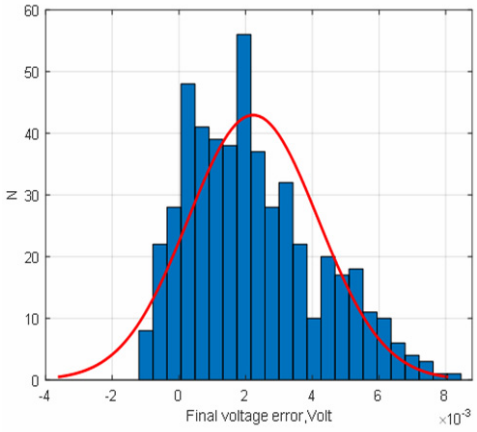

d)

Figure 6. Histograms of final errors from 500 Monte-Carlo simulations; (a) ball position errors; (b) ball velocity errors; (c) coil current errors; (d) coil voltage errors

Table 4. Statistics for state and input errors under initial ball position and input voltage disturbances.

State error	Mean value	Standard deviation	Minimum value	Maximum value
$\Delta y\ (m)$	0.000006	0.000005	-0.0000024	0.000172
$\Delta v\ (m/\sec)$	-0.00042	0.00037	-0.001252	0.00019
$\Delta i\ (Amp)$	0.00361	0.00334	-0.00134	0.00988
$\Delta V\ (Volt)$	0.00343	0.002962	-0.00117	0.008499

In summary, the adaptive algorithm has successfully led the system to the desired values despite the wide range of dispersions of initial ball positions and coil voltages.

Figures 6(a)-6(c) present the statistical results of the final ball position error, final ball velocity error, final coil current error, and final coil voltage error, respectively. Figure 6 and Table 4 summarize the Monte-Carlo simulation results. These statistical results demonstrate that the minimum and maximum values are nearly close to the steady-state conditions, and all the standard deviations are insignificant. Thus, the simulated results illustrate the effectiveness and ability of the proposed algorithm to stabilize the magnetic suspension system.

6.1.3 Initial Ball Position, Steady State Ball Position, and Ball Mass Disturbances

Next, we implemented a Monte-Carlo simulation consisting of 500 suspension system trajectories with random dispersions in the initial ball position, steady-state ball position, and ball mass. The random states have uniform distributions with mean values equal to the nominal states shown in Table 5. Limits for the uniform distributions are ±50 % from the nominal values for initial ball position and steady-state position and ± 66.7 % for ball mass as shown in Table 5.

Figures 7(a)-7(c) present the 500 trials of ball position, ball velocity, coil current histories, respec–tively. These figures match the steady-state conditions well in the presence of large dispersions of the initial ball position, steady-state ball position, and suspended mass uncertainties Although the ball position, coil current, and coil voltage show different final values in different simulations Eq. (15), they reach the zero ball velocity at the steady-state condition. Figure 7(a) was obtained to be feasible because all of the ball position profiles track the references perfectly within the interval [0 - 0.1] m. Figure 7(d) shows 500 closed-loop voltage histories. As seen from Fig. 7(d), the steady-state time and overshoot vary due to the variation of system inputs. This figure shows that the actual trajectories track the steady-state references and satisfy the closed-loop voltage limitation. In summary, the adaptive algorithm has successfully led the system to the desired values despite the wide range of dispersions of initial ball position, steady-state ball position, and ball mass.

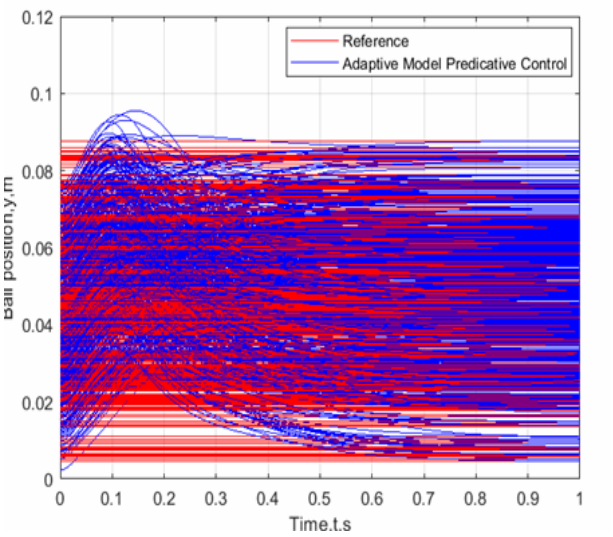

a)

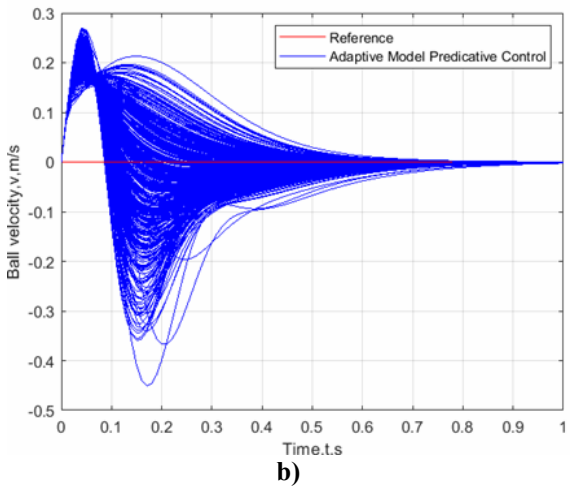

b)

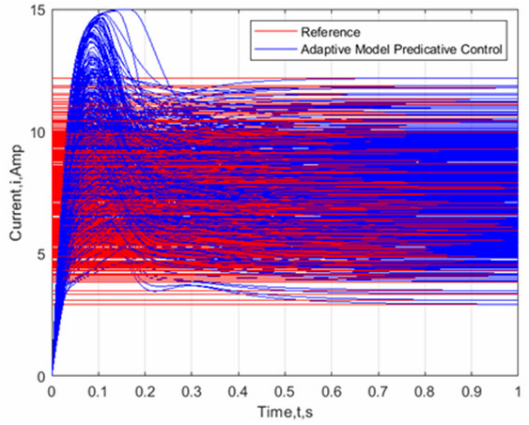

c)

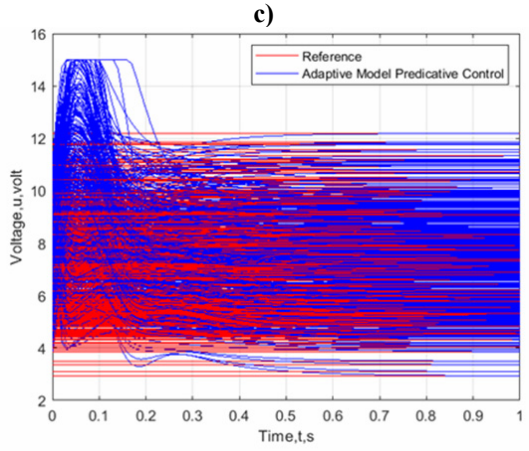

d)

Figure (7) Off-nominal magnetic profiles with dispersions of initial ball position, ball mass, and steady-state position; (a) ball position vs. time; (b) ball velocity vs. time; (c) coil current vs. time; (d) coil voltage vs. time

Table 5: Uncertain System Parameters

System Parameter	Nominal value	Maximum value	Minimum value
Initial ball position (m)	0.04	0.08	0
Steady state position (m)	0.045	0.09	0
Ball mass(kg)	0.15	0.25	0.05

Figures 8(a)-8(c) present the statistical results of the final ball position error, final ball velocity error, final coil current error, and final coil voltage error, respec–tively. Figure 8 and Table 6 summarize the Monte-Carlo simulation results. These statistical results demonstrate that the minimum and maximum values are nearly close to the steady-state conditions, and all the standard deviations are insignificant. Thus, the simulated results illustrate the effectiveness and ability of the proposed algorithm to stabilize the magnetic suspension system.

Table 6. Statistics for state and input errors under initial ball position, steady-state ball position, and ball mass disturbances

State error	Mean value	Standard deviation	Minimum value	Maximum value
$\Delta y\ (m)$	0.000007	0.000006	-0.0000074	0.000346
$\Delta v\ (m/\sec)$	-0.00053	0.00039	-0.00272	0.00049
$\Delta i\ (Amp)$	0.00462	0.0013	-0.00482	0.0244
$\Delta V\ (Volt)$	0.001224	0.0029512	-0.0041	0.0191

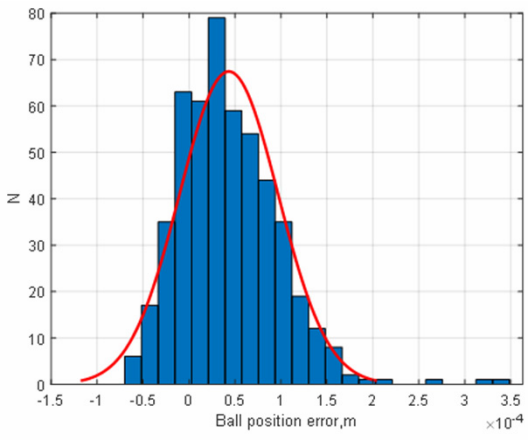

a)

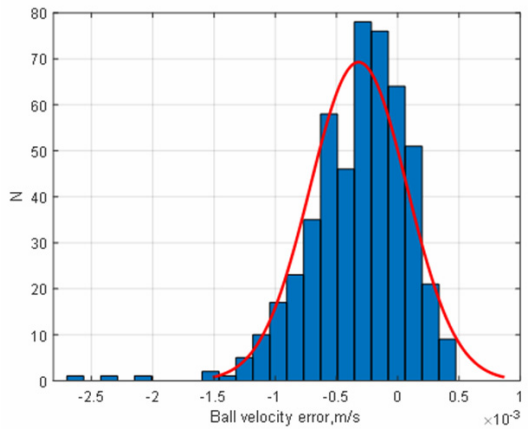

b)

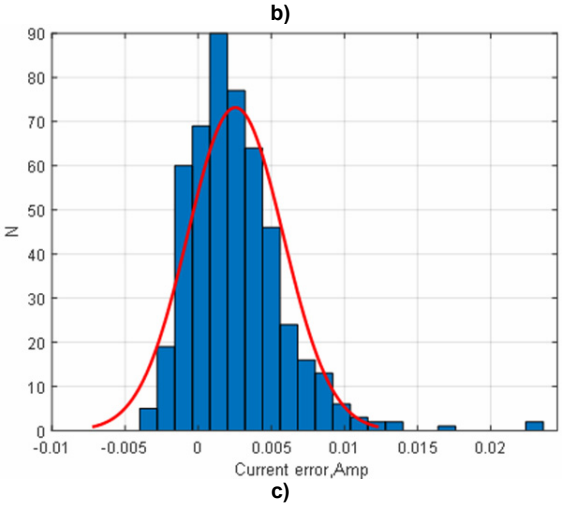

c)

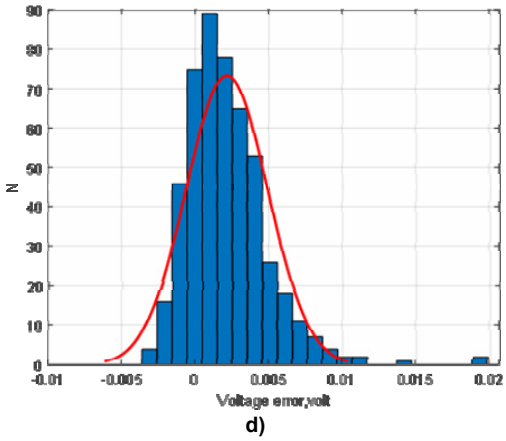

d)

Figure 8. Histograms of final errors from 500 Monte-Carlo simulations; (a) ball position errors; (b) ball velocity errors; (c) coil current errors; (d) coil voltage errors

7. CONCLUSIONS

A new algorithm for the magnetic suspension system has been developed. The steady-state condition served as the reference profile for ball position, ball velocity, and coil current. The closed-loop command was designed instantaneously based on the current discrete system and the operating conditions using the adaptive model predictive control method. The proposed algorithm was tested in the presence of nominal and off-nominal conditions. First, under the nominal conditions, the peak of the ball position response (overshoot) was relatively small and the system needed only 0.65 sec to reach the desired profile for all system states. Second, under the consequent input disturbances, the algorithm was successfully able to stabilize the system quickly with a lower overshoot. Eventually, under the wide range of the system parameters dispersions, the reference profiles were tracked perfectly by the actual profiles without exceeding the state and input constraints. Finally, the Monte-Carlo simulation results performed the effectiveness and robustness of the proposed algorithm.

REFERENCES

[1] Kaplan, B.Z. Regev, D. (1976). Dynamic stabili–zation of tuned circuit levitators. IEEE Transactions on Magnetics 12 (5), 556–559.

[2] Dussaux, M. (1990). Status of the industrial applications of the active magnetic bearings technology. In ASME 1990 International Gas Turbine and Aero-engine Congress and Exposition. American Society of Mechanical Engineers.

[3] Bencze, W. J., Xiao, Y. M., Hipkins, D.N., Franklin, G.F., and Parkinson, B.W. (1996). Gyroscope spin axis direction control for the gravity probe b satellite. In Decision and Control, 1996., Proceedings of the 35th IEEE Conference on, volume 1, 480–485. IEEE.

[4] Hu, S.Y. (2008). Magnetic levitation weight reduction structure for a vertical wind turbine generator. US Patent 7, 462,950.

[5] Kumbernuss, J., Jian, C.,Wang, J.,Yang, H., and Fu,W.(2012). A novel magnetic levitated bearing system for vertical axis wind turbines (vawt).Applied Energy, 90(1), 148–153.

[6] M. Ono, S. Koga, and H. Ohtsuki, “Japan’s superconducting Maglev train,” IEEE Instrum. Meas. Mag, vol. 5, no. 1, pp. 9–15, Mar. 2002.

[7] D. M. Rote and Y. Cai, “Review of dynamic stability of repulsive force Maglev suspension systems,” IEEE Trans. Magn, vol. 38, no. 2, pp.1383–1390, Mar. 2002.

[8] M. Y. Chen, M. J. Wang, and C. L. Fu, “A novel dual-axis repulsive Maglev guiding system with permanent magnet: Modeling and controller design,” IEEE/ASME Trans. Mechatronics, vol. 8, no. 1, pp.77–86, Mar. 2003.

[9] Kaloust, J., C. Ham, J. Siehling, E. Jongekryg, and Q. Han. "Nonlinear robust control design for levitation and propulsion of a maglev system." IEE Proceedings-Control Theory and Applications 151, no. 4 (2004): 460-464.

[10] Barie, W. and Chiasson, J. (1996). Linear and nonlinear state-space controllers for magnetic levitation. International Journal of systems science, 27(11), 1153–1163.

[11] El Hajjaji, A. and Ouladsine, M. (2001). Modeling and nonlinear control of magnetic levitation systems. IEEE Transactions on Industrial Electronics, 48(4), 831–838.

[12] Isidori, A. (2013). Nonlinear control systems. Springer Science & Business Media.

[13] D. L. Trumper, S. M. Olson, and P. K. Subrahmanyan, “Linearizing control of magnetic suspension systems,” IEEE Trans. Control Syst. Technol. vol. 5, no. 4, pp. 427–438, Jul. 1997.

[14] A. E. Hajjaji and M. Ouladsine, “Modeling and nonlinear control of magnetic suspension systems,” IEEE Trans. Ind. Electron., vol. 48, no.4, pp. 831–838, Aug. 2001.

[15] W. G. Hurley and W. H. Wolfle, “Electromagnetic design of a magnetic suspension system,” IEEE Trans. Educ, vol. 40, no. 2, pp.124–130, May 1997.

[16] J. Joo and J. H. Seo, “Design and analysis of the nonlinear feedback linearizing control for an electromagnetic suspension system,” IEEE Trans. Control Syst. Technol. vol. 5, no. 1, pp. 135–144, Jan. 1997.

[17] W. G. Hurley and W. H. Wolfle, “Electromagnetic design of a magnetic suspension system,” IEEE Trans. Educ, vol. 40, no. 2, pp.124–130, May 1997.

[18] Yang, Zi-Jiang, and Michitaka Tateishi. "Adaptive robust nonlinear control of a magnetic levitation system." Automatica 37, no. 7 (2001): 1125-1131.

[19] Nataraj, P., Patil, M.D. (2008). Robust control design for nonlinear magnetic levitation system using quantitative feedback theory (qft). In Annual IEEE conference, INDICON 2008, volume 2, 365–370.

[20] Nataraj, P. and Patil, M.D.(2010). Nonlinear control of a magnetic levitation system using quantitative feedback theory (qft). In Reliability, Safety and Hazard (ICRESH), 2010 2nd International Conference on, 542–547. IEEE.

[21] Khimani, D., Rokade, R.(2017). Implementation of sliding mode control on magnetic levitation system. In Advances in Computing, Communication, and Control (ICAC3), volume5, 1–5. IEEE.

[22] Coşkun, S . (2020). Dynamic output-feedback H_∞ control design for ball and plate system. Cumhuriyet Science Journal , 41 (2), 534-541. DOI: 10.17776/csj.672716.

[23] Mercado-Uribe, A, Moreno, JA. Homogeneous integral controllers for a magnetic suspension system. Control Eng Pract 2020; 97: 104325. DOI:10.1016/j. conengprac. 2020. 104325.

[24] Mercado-Uribe JA, Moreno JA (2020). Discontinuous integral action for an arbitrary relative degree in sliding-mode control. Automatica. 118:109018.

[25] Zhou, Ran et al. 'Suspension Characteristics of a Zero-power Permanent Magnetic Suspension System with Flux Path Control'. 1 Jan. 2020: 187 – 198.

[26] Rašuo, B., Bengin, A.: Optimization of Wind Farm Layout, FME Transactions, Vol. 38, No 3, pp 107-114,2010.

[27] Rašuo, B., Dinulović, M., Veg, A., Grbović, A., Bengin, A.: Harmonization of new wind turbine rotor blades development process: A review, Renewable and Sustainable Energy Reviews, Volume 39, November 2014, pp. 874-882, doi: 10.1016/j.rser.2014.07.137

[28] Ocokoljić, G., Rašuo, B., Kozić, M.: Supporting system interference on aerodynamic characteristics of an aircraft model in a low-speed wind tunnel, Aerospace Science and Technology, Vol. 64, May 2017, pp. 133-146, doi: 10.1016/j.ast.2017.01.021.

[29] Ocokoljic, G., Damljanovic, D., Vukovic, D., Rasuo, B.: Contemporary Frame of Measurement and Assessment of Wind-Tunnel Flow Quality in a Low-Speed Facility, FME Transactions, Vol. 46, No. 4, pp.429-442, 2018.

[30] Ocokoljić, G., Damljanović, D., Rašuo, B., Isaković, J.: Testing of a standard model in the VTI's large subsonic wind-tunnel facility to establish users' confidence, FME Transactions, Vol. 42, No. 3, pp. 212-217,2014.

[31] Damlanović, D., Vuković, Dj., Ocokoljić, G., Rašuo, B.: Convergence of transonic wind tunnel test results of the AGARD-B standard model, FME Transactions, Vol. 48, No. 4, pp. 761-769, 2020.

[32] Damlanović, D., Vuković, Dj., Ocokoljić, G., Rašuo, B.: Convergence of transonic wind tunnel test results of the AGARD-B standard model, FME Transactions, Vol. 48, No. 4, pp. 761-769, 2020.

[33] Khalil, Hassan K., and Jessy W. Grizzle. Nonlinear systems. Vol. 3. Upper Saddle River, NJ: Prentice hall, 2002.

[34] Adetola, Veronica, Darryl DeHaan, and Martin Guay. "Adaptive model predictive control for constrained nonlinear systems." Systems & Control Letters 58, no. 5 (2009): 320-326.

[35] Varga, A., 1997. Periodic Lyapunov equations: some applications and new algorithms. International Journal of Control, 67(1), pp.69-88.

[36] F. Al-Bakri, M. Laheeb, K. Salwan. "Online algorithm for controlling an inverted pendulum system under uncertainty in design parameters and initial conditions using Monte-Carlo simulation." In 2018 IEEE 8th Annual Computing and Communication Workshop and Conference (CCWC), pp. 1-7. IEEE, 2018.

[37] Laheeb, Muhi, Khafaji Salwan, Al-Bakri Fawaz, and Lami Sarah. "Online algorithm for controlling a cruise system under uncertainty in design parameters and environmental conditions using Monte-Carlo simulation." In 2018 IEEE 8th Annual Computing and Communication Workshop and Conference (CCWC), pp. 424-430. IEEE, 2018.

[38] Ali H, Fales R (2020) Robust control design for an inlet metering velocity control system of a linear hydraulic actuator. Int J Fluid Power, https://doi.org/10.13052/ijfp1439-9776.2113.

NOMENCLATURE

$L(y)$, Lo, $L1$	Positive constants
$i(t)$	Coil current
m	Ball mass
g	Gravitational acceleration
R	Circuit resistance
y	The position of the ball
f	Magnetic force
ϕ	Magnetic flux
k	Viscous friction
x_1, x_2,x_3	System states
u	System input
A, B	Matrices for linearization
E	Electrical energy
v_{ss}	Steady-state velocity
y_{ss}	Steady-state position
V_{ss}	Steady-state voltage
i_{ss}	Steady-state current
Q	Weight matrix for the states
$\Re$	Weight matrix for the input
$\bar{Q}$	Block diagonal matrix for states
$\bar{R}$	Block diagonal matrix for input
H	Positive-definite Hessian matrix
F	Model predictive gain

ПРЕДИКТИВНА КОНТРОЛА АДАПТИВНОГ МОДЕЛА ЗА СИСТЕМ МАГНЕТНОГ ВЕШАЊА ПОД ДИСПЕРЗИЈАМА ПОЧЕТНЕ ПОЗИЦИЈЕ И ПОРЕМЕЋАЈИМА НАПОНА

Ф.Ф. Ал-Бакри, С.О.В. Кафаци, Х.Х. Али

У раду се разматра нелинеарни систем маг–нетног ослањања који се састоји од механичког кретања и електромагнетног кола. Представљен је онлајн алгоритам који се користи за стабилизацију суспендоване масе циљајући жељену позицију лопте, брзину лопте и струју завојнице. Стање стационарног стања, у коме су положај лопте, брзина лопте и струја завојнице претпостављени константни, коришћен је као референтна путања за симулације затворене петље.

Метода предвиђања адаптивног модела коришћена је за контролу напона завојнице, док су модел дискретног постројења и радни услови мењани у сваком временском кораку. Ефикас–ност предложеног закона управљања је потвр–ђена у присуству поремећаја у почетној позицији лопте, стабилном положају лопте, сус–пендованој маси и напону коришћењем методе Монте-Карло симулације. Синусоидни, степе–насти и импулсни напонски поремећаји приме–њени су последично на систем док су наметнуте насумичне дисперзије почетне позиције лопте. Нумерички резултати са пет стотина покушаја су илустровали да дизајнирани

алгоритам може стабилизовати систем и пратити жељену референцу без прекорачења стања и улазних ограничења упркос широком опсегу дисперзија у почетној позицији лопте, стабилном положају лопте, суспендованој маси и улазном напону сметње.